

Modular Mesoionics: Understanding and Controlling Regioselectivity in 1,3-Dipolar Cycloadditions of Münchnone Derivatives

Marie S. T. Morin,[†] Daniel J. St-Cyr,^{†,||} Bruce A. Arndtsen,^{*,†} Elizabeth H. Krenske,^{*,‡,§} and K. N. Houk^{*,||}

[†]Department of Chemistry, McGill University, 801 Sherbrooke Street West, Montréal, Quebec H3A 2K6, Canada

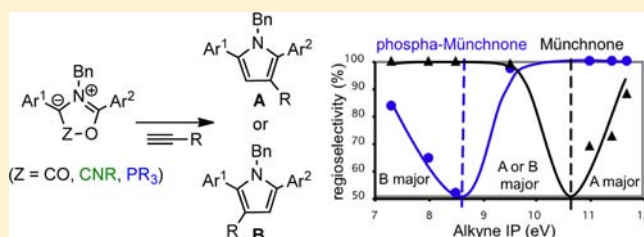
[‡]School of Chemistry, The University of Melbourne, VIC 3010, Australia, and Australian Research Council Centre of Excellence for Free Radical Chemistry and Biotechnology

[§]School of Chemistry and Molecular Biosciences, The University of Queensland, Brisbane, Queensland 4072, Australia

^{||}Department of Chemistry and Biochemistry, University of California, Los Angeles, California 90095, United States

Supporting Information

ABSTRACT: 1,3-Dipolar cycloadditions of mesoionic 1,3-dipoles (Münchnones, imino-Münchnones, and phosphamünchnones) with alkynes offer versatile, modular synthetic routes to pyrroles. Reactivity and regioselectivity differ markedly for different members of this series, and we report here the first general rationale for differences in reactivity by means of a systematic investigation of 1,3-dipolar cycloadditions involving electron-poor and electron-rich alkynes. Competition kinetic measurements indicate that Münchnones and phosphamünchnones are nucleophilic 1,3-dipoles that react most rapidly with electron-poor alkynes. However, the regioselectivities of cycloadditions are found to undergo an inversion as a function of alkyne ionization potential. The exact point at which this occurs is different for the two dipoles, allowing rational control of the pyrrole formed. The origins of these reactivities and regioselectivities are examined computationally. Frontier molecular orbital predictions are found not to be accurate for these reactions, but transition state calculations give correct predictions of reactivity and selectivity, the origins of which can be analyzed using the distortion/interaction model of reactivity. Cycloadditions with electron-poor alkynes are shown to favor the regioisomer that has either the most favorable TS interaction energy (Münchnones or imino-Münchnones) or the smallest TS distortion energy (phosphamünchnones). Cycloadditions with more electron-rich aryl-substituted alkynes, on the other hand, generally favor the regioisomer that has the smaller TS distortion energy. These insights delineate the synthetically important distinctions between Münchnones and phosphamünchnones: phosphamünchnones undergo highly regioselective cycloadditions with electron-poor alkynes that do not react selectively with Münchnones, and the reverse is true for cycloadditions of Münchnones with electron-rich alkynes.



INTRODUCTION

1,3-Dipolar cycloadditions of Münchnones (1,3-oxazolium-5-oxides) (1), imino-Münchnones (2), and phosphamünchnones (3) (also known as Montréalones) (Figure 1) with alkynes provide convenient access to pyrroles. Despite sharing a common azomethine ylide motif, these three classes of mesoionic 1,3-dipoles display varied reactivities and regioselectivities that were not previously systematized or explained.¹

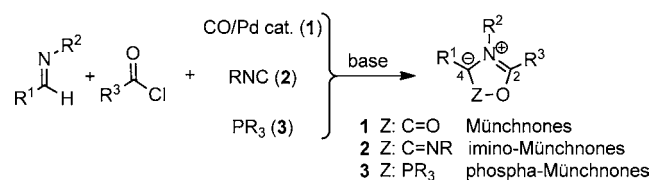


Figure 1. Mesoionic 1,3-dipoles: Münchnones (1), imino-Münchnones (2), and phosphamünchnones (3).

In this paper, we report experimental and theoretical investigations that delineate the differences in behavior between the three classes of 1,3-dipoles in their cycloadditions with alkynes. Our results provide a unifying picture of the factors that control reactivity and selectivity in the cycloadditions of mesoionic dipoles, which has predictive utility for regioselective construction of pyrroles.

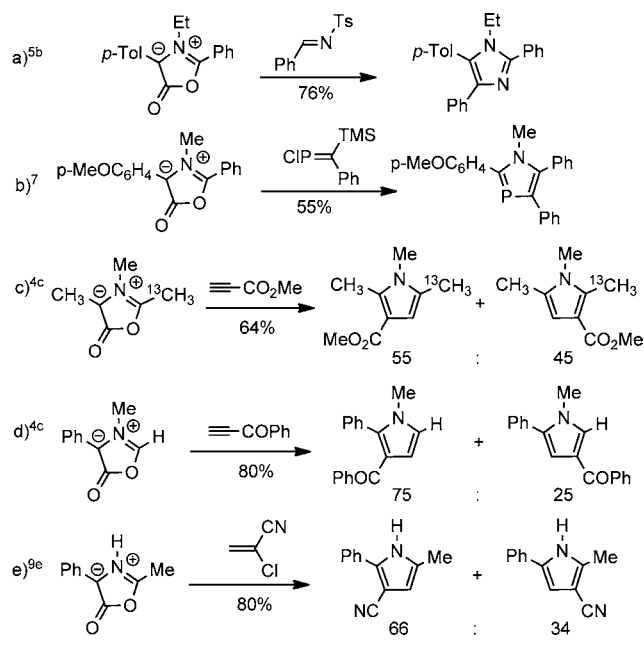
Münchnone cycloaddition was first reported by Huisgen in 1964.² Upon treatment with alkynes, they undergo 1,3-dipolar cycloaddition accompanied by CO₂ loss to form pyrroles. Subsequent studies extended the scope of Münchnone cycloadditions to include many other dipolarophiles, providing attractive routes to pyrrolines, imidazoles, imidazolines, and other heterocycles.³ Münchnones react most rapidly with electron-poor dipolarophiles. This “Type I” Sustmann behavior

Received: July 4, 2013

Published: October 17, 2013

suggests a predominant frontier molecular orbital (FMO) interaction between HOMO (Münchnone) and LUMO (dipolarophile).⁴ FMO calculations predict that the favored regioisomer of cycloaddition should be the one where the nucleophilic C4 carbon of the Münchnone has bound to the electrophilic terminus of the dipolarophile.⁵ However, the regioselectivities of Münchnone cycloadditions with alkynes are often found to be poor. Whereas cycloadditions with electronically biased dipolarophiles such as imines,⁶ aldehydes,⁷ and phosphalkenes⁸ do give the predicted cycloadduct with high selectivity (e.g., Scheme 1a and 1b), cycloadditions with

Scheme 1. Examples of Münchnone Regioselectivity in Cycloaddition Reactions



polarized alkynes^{5b,c,9} and alkenes^{5d,10} frequently lead to mixtures of regioisomers (e.g., Scheme 1c–e). A number of attempts have been made to understand this selectivity^{5,11} and have proposed explanations based on steric influences and cycloaddition asynchronicity. However, it remains unclear why Münchnones do not show the same degree of selectivity in their reactions with alkynes as they do in their reactions with other electronically biased dipolarophiles.

For the purpose of controlling regioselectivity, substituent effects at positions R¹ and R³ in Münchnones are not generally useful, as they are frequently small and/or complicated by steric effects. A better alternative would be to tune the group “Z” (Figure 1). Imino-Münchnones (2, Z = C=NR) were first reported in 1968.¹² Phospha-Münchnones (3, Z = PR₃) are much more recent, having been reported for the first time by us in 2007.¹³ Phospha-Münchnones have reactivity profiles quite different from Münchnones and imino-Münchnones. They have also been called “Montréalones” in light of their discovery in Montréal, as Huisgen named Münchnones after München where they were developed and Earl¹⁴ named “Sydnones” after Sydney. The efficiencies of phospha-Münchnone cycloadditions with alkenes¹⁵ or alkynes^{13a,b,d} depend strongly on the identity of PR₃. While PPh₃ is not effective, a PPh(catechyl) unit allows rapid and high-yielding cycloadditions. Each of these three classes of mesoionic 1,3-dipoles—Münchnones, imino-Münchnones, and phospha-Münchnones—can be synthesized in a

one-pot, multicomponent procedure, starting from an imine (R¹HC=NR²), an acid chloride (R³COCl), and either CO/Pd (for 1),¹⁶ RNC (for 2),¹⁷ or PR₃ (for 3).^{13a,b}

Here we used these modular assembly routes to prepare Münchnone derivatives differing only in the group Z, and we investigated their 1,3-dipolar cycloadditions with electron-poor and electron-rich alkynes. The patterns of reactivity and selectivity are examined and explained by means of density functional theory calculations. Our results indicate that these different classes of mesoionic dipoles provide complementary opportunities for pyrrole synthesis: a C=O (or C=NR) Z group allows regioselective cycloadditions with electron-rich alkynes, while switching to a PR₃ group allows regioselective cycloadditions with electron-poor alkynes.

RESULTS AND DISCUSSION

Experimental Measurements of Cycloaddition Regioselectivities and Reactivities. We prepared three 1,3-dipoles—Münchnone 1a, imino-Münchnone 2a, and phospha-Münchnone 3a—from (*p*-tolyl)HC=NBn, *p*-MeOC₆H₄COCl, and the appropriate “Z” unit.¹⁸ The *p*-tolyl (*p*-Tol) and *p*-methoxyphenyl (PMP) groups were chosen in order to minimize the regiochemical influences of the groups at the C2 and C4 positions.¹⁹ The regioselectivities of the 1,3-dipolar cycloadditions of 1a–3a with alkynes were measured by in situ ¹H NMR spectroscopy and isolation and full characterization of the pyrrole products. Results are given in Tables 1 and 2.

1. Electron-Poor Alkynes. Table 1 summarizes cycloadditions of the 1,3-dipoles with electron-poor alkynes (4a–4d). Reactions of Münchnone 1a and imino-Münchnone 2a with alkynes 4a–4d gave regioisomeric mixtures favoring pyrrole A (69:31–93:7). Reactions of phospha-Münchnone 3a, on the other hand, gave pyrrole A as the only observable regioisomer (>95:5). The Münchnone usually gave lower selectivities than the imino-Münchnone. For example, cycloaddition of 1a with methyl propiolate (4a) yielded a 73:27 mixture of A and B (entry 1), while 2a gave an 88:12 mixture (entry 2). Changing to the internal alkyne 4b (entries 4–6) led to an increase in selectivity with 1a but no change in selectivity from 2a or 3a. This rules out the possibility that the regioselectivities obtained with 4a were due simply to a preference for addition of the nucleophilic C4 carbon to the less sterically hindered alkyne terminus. Cycloadditions involving the less electron-poor alkyne 4c gave lower selectivity with the Münchnone but no changes in selectivity for the imino- or phospha-Münchnone (entries 7–9). Conversely, the most electron-poor alkyne 4d gave the highest selectivities overall (entries 10–12). In this case, even the Münchnone gave a synthetically useful level of regioselectivity.

The general trend in these cycloadditions with electron-poor alkynes is toward higher regioselectivity in the order 1a < 2a < 3a. Thus, replacing the carbonyl group by PPh(catechyl) appears to generate a more electron-rich or electronically biased dipole. Experimental evidence for the greater nucleophilicity of the phosphorus-containing dipole was obtained from the competition experiments shown in Figure 2. Treatment of a 1:1 mixture of 1a and 3a with 0.4 equiv of either methyl propiolate (4a) or dimethyl propiolamide (4c) led to consumption of only the phospha-Münchnone; the Münchnone failed to react. These results imply that the phospha-Münchnone is >20 times more reactive than the Münchnone toward 4a or 4c.

Table 1. Cycloadditions of Mesoionic 1,3-Dipoles with Electron-Poor Alkynes^a

1a Z: C=O
2a Z: C=N(Cyclohexyl)
3a Z: PPh(Catechyl)

Entry	Alkyne	1,3-Dipole	Yield ^b	Ratio ^c A : B
1	\equiv -CO ₂ Me 4a	1a	65 %	73 : 27
2	\equiv -CO ₂ Me 4a	2a	85 %	88 : 12
3	\equiv -CO ₂ Me 4a	3a	91 %	> 95 : 5
4 ^d	\equiv -CO ₂ Me 4b	1a	63 %	91 : 9
5 ^d	\equiv -CO ₂ Me 4b	2a	21 %	87 : 13
6 ^d	\equiv -CO ₂ Me 4b	3a	45 %	> 95 : 5
7	\equiv -C(=O)NMe ₂ 4c	1a	95 %	69 : 31
8	\equiv -C(=O)NMe ₂ 4c	2a	35 %	89 : 11
9	\equiv -C(=O)NMe ₂ 4c	3a	98 %	> 95 : 5
10	\equiv -C(=O)O-C ₆ H ₄ -CF ₃ 4d	1a	76 %	88 : 12
11	\equiv -C(=O)O-C ₆ H ₄ -CF ₃ 4d	2a	84 %	93 : 7
12	\equiv -C(=O)O-C ₆ H ₄ -CF ₃ 4d	3a	99 %	> 95 : 5

^a1a or 3a (0.1 mmol), alkyne (0.2 mmol), CDCl₃ (1 mL), rt, 10 min to 2 days; 2a (in situ, 0.2 mmol), alkyne (0.6 mmol), CDCl₃ (1.5 mL), rt, 1–15 days. ^bNMR. ^cBy ¹H NMR of reaction mixture. ^dAt 85 °C.

II. Electron-Rich Alkynes. Cycloadditions with arylacetylenes (**4e–4h**) displayed quite different regioselectivities from those with the electron-poor alkynes (Table 2). Because Münchnone **1a** and phosphamünchnone **3a** displayed the most divergent selectivities toward the electron-poor alkynes above, we employed only these two dipoles in our investigations with the aryl-substituted alkynes. Cycloadditions of the Münchnone with the arylacetylenes displayed consistently high regioselectivities favoring pyrrole B (A:B < 5:95). In contrast, the regioselectivities obtained with the phosphamünchnone were variable. Reaction with phenylacetylene (**4e**) gave a ca. 1:1 mixture of A and B (entry 2), while reaction with the less electron-rich arylacetylene **4f** gave exclusively A (entry 4), and reaction with the more electron-rich alkynes **4g** and **4h** gave predominantly B (entries 6 and 8). Interestingly, the Münchnone and phosphamünchnone show completely opposite selectivities toward alkyne **4f**.

Competition studies (Figure 2) indicated that phosphamünchnone **3a** reacted faster than Münchnone **1a** with the arylacetylene **4f**, although the reactivities differed only by a factor of 2.3, compared with >20 for the electron-poor alkynes **4a** and **4c**. Furthermore, the Münchnone reacted at least 20 times faster than the phosphamünchnone in the cycloaddition with electron-rich arylacetylene **4e**.

Table 2. Cycloadditions of Mesoionic 1,3-Dipoles with Arylacetylenes^a

1a Z: C=O
3a Z: PPh(Catechyl)

Entry	Alkyne	1,3-Dipole	T [°C]	Yield ^b	Ratio ^c A : B
1	\equiv -Ph 4e	1a	rt	40 %	< 5 : 95
2	\equiv -Ph 4e	3a	70	58 %	48 : 52
3	\equiv -C ₆ H ₄ (CF ₃) ₂ 4f	1a	rt	64 %	< 5 : 95
4	\equiv -C ₆ H ₄ (CF ₃) ₂ 4f	3a	rt	86 %	> 95 : 5
5	\equiv -C ₆ H ₄ OMe 4g	1a	rt	38 %	< 5 : 95
6	\equiv -C ₆ H ₄ OMe 4g	3a	70	36 %	35 : 65
7	\equiv -C ₆ H ₄ NMe ₂ 4h	1a	rt	30 %	< 5 : 95
8	\equiv -C ₆ H ₄ NMe ₂ 4h	3a	70	28 %	16 : 84

^aConditions of Table 1. ^bIsolated yield. ^cDetermined by ¹H NMR of crude reaction mixture.

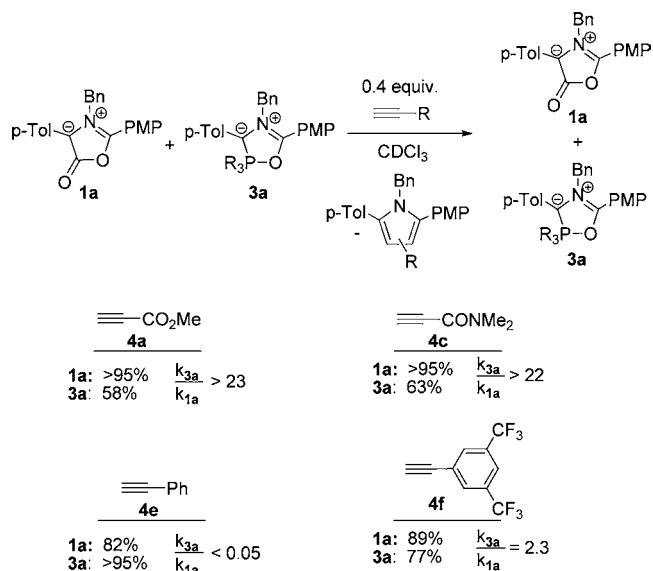


Figure 2. Competition reactions of Münchnone **1a** and phosphamünchnone **3a** with alkynes. Data show the amounts of each 1,3-dipole remaining after treatment of an equimolar mixture with 0.4 equiv of alkyne. Relative rates were calculated as in ref 20.

III. Reactivity/Selectivity Relationship. To quantify reactivity/selectivity relationships for dipoles **1a** and **3a**, we measured the kinetics of cycloadditions with alkynes **4a,c–h** by means of competition reactions. Relative rate constants are listed in Table 3, and reactivity/selectivity data are plotted in Figure 3 as a function of alkyne ionization potential.²¹

Table 3. Relative Rate Constants of 1,3-Dipolar Cycloadditions of 1a and 3a with Alkynes^a

Alkyne	k_{rel} of cycloaddition with 1a	k_{rel} of cycloaddition with 3a
4-(Me) ₂ NC ₆ H ₄ -≡ 4h	1	1
4-MeOC ₆ H ₄ -≡ 4g	1.2 (± 0.3)	4.4 (± 0.7)
Ph-≡ 4e	1.8 (± 0.2)	14.0 (± 1.5)
3,5-(CF ₃) ₂ C ₆ H ₄ -≡ 4f	17.0 (± 1.5)	653 (± 49)
≡-CONMe ₂ 4c	107 (± 12)	13.9 (± 0.8) × 10 ⁴
≡-CO ₂ Me 4a	15.5 (± 1.2) × 10 ²	4.94 (± 0.37) × 10 ⁶
≡-CO ₂ (4-CF ₃ C ₆ H ₄) 4d	3.2 (± 0.3) × 10 ⁴	3.90 (± 0.34) × 10 ⁷

^aDetermined by competition reactions of 1a or 3a (0.1 mmol) with two different alkynes (0.5–2.0 mmol)²⁰ and ¹H NMR analysis of the resulting pyrroles. Error in rates relative to alkyne above in the table, and calculated from the average of two experiments using standard 5% error in ¹H NMR integration.

For both 1,3-dipoles, the rate of cycloaddition increases with alkyne ionization potential. This can be clearly seen in the plot of relative reactivities in Figure 3a. Both 1,3-dipoles show a roughly linear correlation between reactivity and alkyne ionization potential as expected for nucleophilic 1,3-dipoles.²² Interestingly, the phospho-Münchnone displays a much wider range of reactivities, reacting over 10⁷ times faster with the very electron poor 4d than with the electron-rich alkyne 4h.

However, contrary to expectation for nucleophilic 1,3-dipoles, plots of regioselectivity against alkyne ionization potential (Figure 3b and 3c) are not linear. Instead, both dipoles show an inversion along the series, favoring pyrrole B at low alkyne IPs and pyrrole A at high alkyne IPs. The regioisomer predicted for a nucleophilic dipole (A) dominates over a wider range of alkynes with the phospho-Münchnone than with the Münchnone. In combination with the linear correlation of reactivity with IP, the observed inversion of regioselectivity with IP does not conform to FMO predictions.²³ Nevertheless, the data clearly show that alkyne cycloaddition regioselectivity can indeed be qualitatively predicted based on alkyne ionization potential. The ionization potential at which selectivity inverts for Münchnones is about 10.7 eV, compared to 8.6 eV for phospho-Münchnones. These differences enable one to synthesize a pyrrole in high regiochemical purity from any of the alkynes examined. For alkyne 4f, the ionization potential (ca. 9.5 eV) lies outside both of the mixture-producing regions yet on opposite sides of the A ↔ B regioisomeric transition points for the two dipoles, allowing both isomers of the pyrrole to be generated in >95% regioisomeric purity from cycloadditions with the two dipoles.

Computational Studies of Regioselectivity and Reactivity. We used density functional theory calculations to examine the mesoionic 1,3-dipoles' reactivities and regioselectivities. Computations were performed at the B3LYP/6-31+G(d) level of theory, which we previously used^{13b,c} to characterize phospho-Münchnone structures and reactivities. Figure 4 shows the FMO energies and π coefficients of model 1,3-dipoles 1b–3b and selected alkynes.

Methyl propiolate (4a) was used as a representative electron-poor alkyne. As has been previously noted for Münchnones,^{5b,c,9a} the FMO picture correctly predicts some, but not all, of the experimental observations. The dominant FMO interaction is HOMO(Münchnone)–LUMO(4a), consistent with the observed preference for pyrrole A in cycloadditions of 3a with electron-poor alkynes 4a–4d (Table 1). The dipole

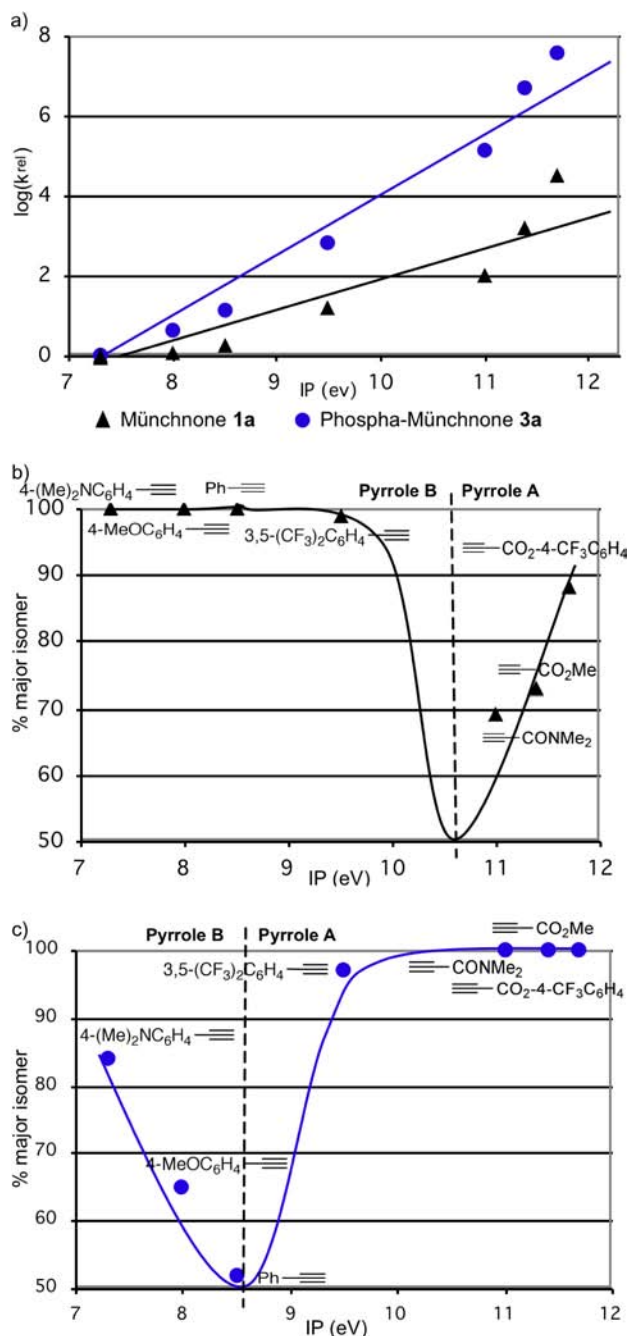


Figure 3. (a) Reactivity and (b and c) selectivity of cycloaddition of (▲) Münchnone 1a and (●) phospho-Münchnone 3a with alkynes as a function of alkyne ionization potential.

HOMO energies correctly predict that an imino-Münchnone should be more regioselective than a Münchnone but fail to predict that a phospho-Münchnone should be more selective than either of these. The HOMO energies also fail to predict that a phospho-Münchnone should react faster than a Münchnone with electron-poor alkynes (Figure 2 and Table 3).

Frontier molecular orbital considerations also give qualitatively inaccurate predictions of regioselectivity for the more electron-rich alkynes 4e, 4f, and 4h. For example, the HOMO energies and coefficients of the Münchnone and phospho-Münchnone are nearly identical, and the phospho-Münchnone has the higher LUMO energy, yet the Münchnone consistently

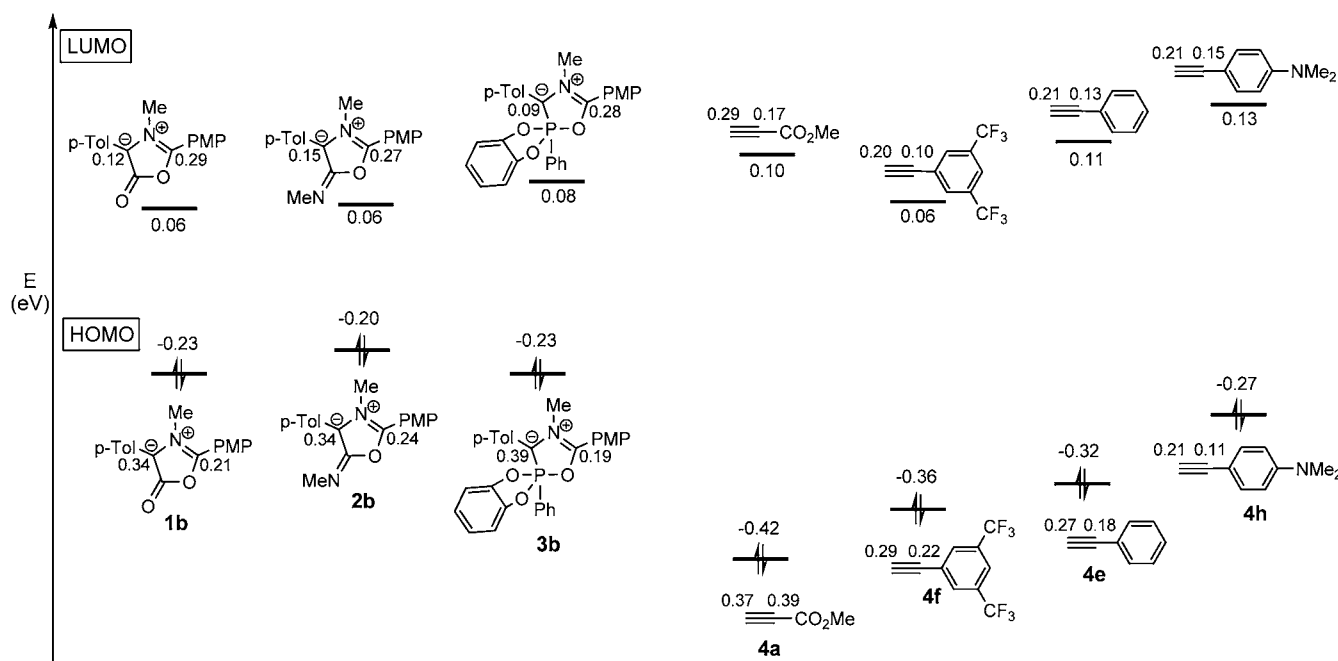


Figure 4. Frontier molecular orbital diagram for 1,3-dipoles **1b**–**3b** and selected alkyne dipolarophiles. Orbital energies (eV) and absolute values of the coefficients at the reacting termini were computed at the HF/6-31G//B3LYP/6-31+G(d) level.

favors pyrrole B experimentally, while the phospho-Münchnone is “ambiphilic”.

Simple FMO considerations are not generally useful for comparing the reactivities and selectivities of cycloadditions involving these mesoionic 1,3-dipoles. We therefore computed transition states for the 1,3-dipolar cycloadditions of model mesoionic 1,3-dipoles with the four alkynes. Figure 5 shows the transition states for cycloadditions of model 1,3-dipoles **1c**–**3c** with methyl propiolate **4a**. Activation barriers for these TSs are listed in Table 4. Activation barriers for cycloadditions involving arylacetylenes, this time with the model 1,3-dipoles **1d** and **3d** (which lack the N-Me group of **1c** and **3c**), are given in Table 5. The tables list the values of ΔH^\ddagger and ΔG^\ddagger in the gas phase as well as solution-phase values of ΔG^\ddagger in chloroform, which were computed using the SMD solvent model. The TS geometries for cycloadditions involving the most electron-rich alkyne, **4h**, are shown in Figure 6. 1,3-Dipolar cycloadditions of these mesoionic 1,3-dipoles with alkynes lead to bicyclic intermediates, which undergo retro-(4 + 2) cycloaddition with extrusion of Z=O (Z=CO or PR₃) to generate the pyrrole. Reaction profiles including both the 1,3-dipolar cycloaddition and the retro-(4 + 2) cycloaddition were computed for four representative cases (**1c/3c** + **4a** and **1d/3d** + **4e**). The reaction profile for **1c** + **4a** is shown in Figure 7. Formation of the bicyclic intermediate **Int-1-a-A** was found to be effectively irreversible, and the intermediate rapidly extrudes CO₂ with a barrier of <1 kcal/mol. Similar features are observed in the corresponding reaction profiles for the other three examples studied (see Supporting Information). Thus, the regioselectivity of pyrrole formation is controlled by the relative energies of the isomeric 1,3-dipolar cycloaddition transition states.

For cycloadditions involving methyl propiolate (Table 4), the gas-phase values of ΔH^\ddagger and ΔG^\ddagger predict the correct sense and degree of regioselectivity (a preference for pyrrole A, which increases in the order **1** < **2** < **3**) and the correct relative rates of cycloaddition (**1** < **3**).²⁴ Theory also predicts the correct regioselectivities for cycloadditions involving arylacetylenes

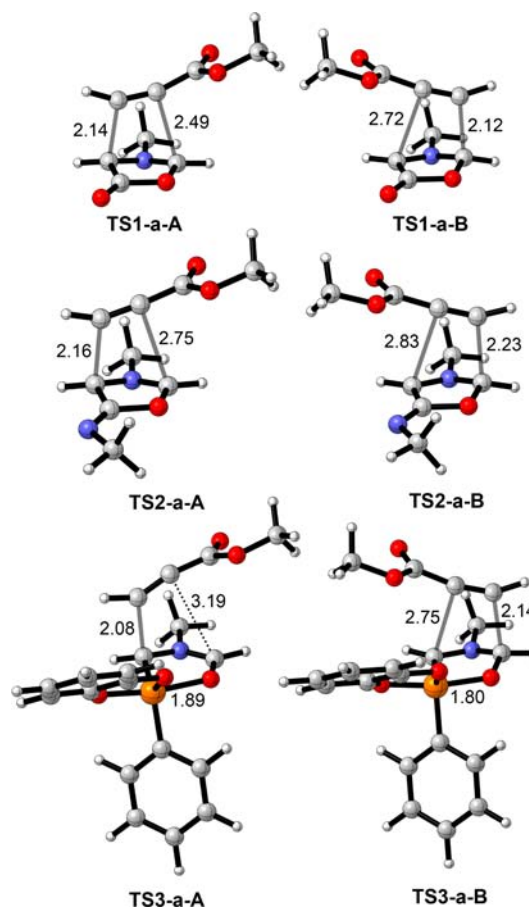
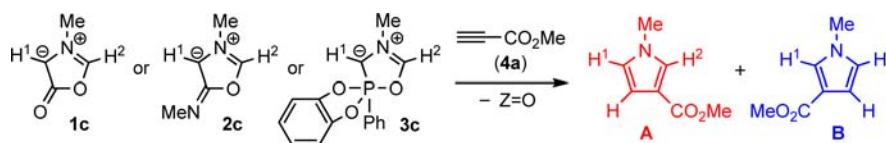


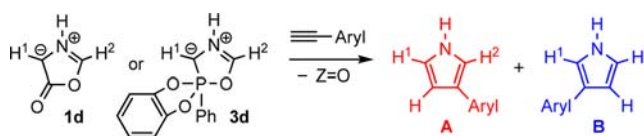
Figure 5. Transition structures for 1,3-dipolar cycloadditions of **1c**–**3c** with methyl propiolate; calculated at the B3LYP/6-31+G(d) level. Distances in Angstroms.

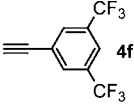
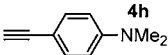
(Table 5). Here, cycloadditions of Münchnone **1a** with arylacetylenes consistently favored pyrrole B experimentally

Table 4. Computed Activation Barriers and Distortion/Interaction Analyses for 1,3-Dipolar Cycloadditions of 1c–3c with Methyl Propiolate^a

1,3-dipole	exptal ^b	ΔH^\ddagger (gas)		ΔG^\ddagger (gas)		ΔG^\ddagger (CHCl ₃)		ΔE_{dist}		ΔE_{int}	
	A:B	A	B	A	B	A	B	A	B	A	B
1c	73:27	10.1	10.4	24.7	25.0	27.5	26.7	21.7	18.6	-12.5	-9.1
2c	88:12	3.7	4.5	17.9	19.0	20.3	21.1	13.8	11.9	-11.2	-8.4
3c	>95:5	8.4	12.2	22.8	28.1	22.4	29.7	15.7	21.3	-8.2	-9.9

^aB3LYP/6-31+G(d), 298.15 K, 1 mol/L, kcal/mol. Solution values incorporate SMD solvation energies in chloroform. ^bExperimental regioisomer ratios for reactions of 1a–3a (from Table 1).

Table 5. Computed Activation Barriers and Distortion/Interaction Analyses for 1,3-Dipolar Cycloadditions of 1d and 3d with Arylacetylenes^a

Alkyne and 1,3-Dipole	Exptal ^b	ΔH^\ddagger (gas)		ΔG^\ddagger (gas)		ΔG^\ddagger (CHCl ₃)		ΔE_{dist}		ΔE_{int}	
	A:B	A	B	A	B	A	B	A	B	A	B
\equiv -Ph 4e											
1d	<5:95	16.9	14.5	31.2	28.8	34.7	31.6	24.8	20.0	-8.9	-6.4
3d	48:52	18.4	18.6	32.7	33.4	35.7	36.0	24.9	23.1	-7.3	-5.2
 4f											
1d	<5:95	15.9	13.6	30.2	28.7	33.2	31.1	23.8	19.8	-8.9	-7.1
3d	>95:5	14.6	16.9	28.7	32.6	29.6	34.9	18.0	23.1	-4.2	-6.8
 4h											
1d	<5:95	17.7	14.3	32.7	28.7	36.6	31.7	25.3	19.4	-8.6	-6.0
3d	16:84	20.1	18.6	35.4	33.8	38.9	36.5	26.7	22.5	-7.4	-4.6

^aB3LYP/6-31+G(d), 298.15 K, 1 mol/L, kcal/mol. Solution values incorporate SMD solvation energies in chloroform. ^bExperimental regioisomer ratios for reactions of 1a and 3a (from Table 2).

(>95:5), and calculations predict pyrrole B to be favored by 2.3–3.4 kcal/mol ($\Delta\Delta H^\ddagger$). Experimentally, phospha-Münchnone **3a** was ambiphilic toward the arylacetylenes, and computed barriers mirror this result by showing a strong preference for pyrrole A with alkyne **4f** ($\Delta\Delta H^\ddagger = 2.3$ kcal/mol), a preference for pyrrole B with **4h** ($\Delta\Delta H^\ddagger = 1.5$ kcal/mol), and low selectivity with **4e** ($\Delta\Delta H^\ddagger = 0.2$ kcal/mol).

Calculations appear to underestimate the reactivity of the phospha-Münchnone relative to the Münchnone in cycloadditions with arylacetylenes. This apparent underestimation stems from the absence of substituents on the carbon and nitrogen atoms of model phospha-Münchnone **3d**. Previously, we showed^{13b,c} that the activation energies for concerted cycloadditions of phospha-Münchnones with ethylene correlate with the length of the P–O bond in the reactant; the longer the P–O bond, the greater the bond must contract before the TS geometry can be reached and the higher the activation energy. The absence of any *N*-alkyl or *C*-aryl substituents on the model phospha-Münchnone **3d** makes the P–O bond 0.13 Å longer than in the substituted analogue **3b** (1.97 vs 1.84 Å), which produces an artificial elevation of the activation barrier. A

similar effect is likely to be present in the reaction of **3c** with methylpropiolate (Table 4).

We also computed the activation barriers at the M06-2X/6-311+G(d,p)//B3LYP/6-31+G(d) level of theory (see Supporting Information). M06-2X calculations agreed quite closely with experiment for methyl propiolate but gave incorrect predictions of regioselectivity for most of the arylacetylene cycloadditions.

To analyze the variations in rates and regioselectivities, we applied the distortion/interaction model²⁵ of reactivity. The right-hand columns in Tables 4 and 5 show the total energy required to distort the 1,3-dipole and alkyne to their transition-state geometries (ΔE_{dist}) and the energy associated with the interaction between the cycloaddends in each TS (ΔE_{int}).

Distortion/interaction analysis shows that, for reactions with methyl propiolate (Table 4), the Münchnone and imino-Münchnone regioselectivities are controlled by the interaction energy. The favored transition states for both of these dipoles (leading to A) have larger distortion energies than the TSs leading to B, but they are lower in energy because they are stabilized by a stronger interaction between the reactants, reflecting the nucleophilic character of the 1,3-dipoles. The

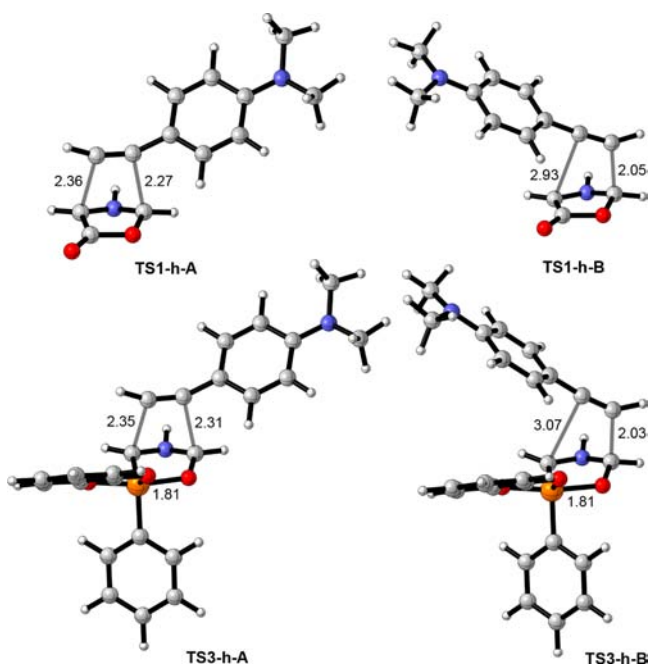


Figure 6. Transition structures for 1,3-dipolar cycloadditions of **1d** and **3d** with alkyne **4h**; calculated at the B3LYP/6-31+G(d) level. Distances in Angstroms.

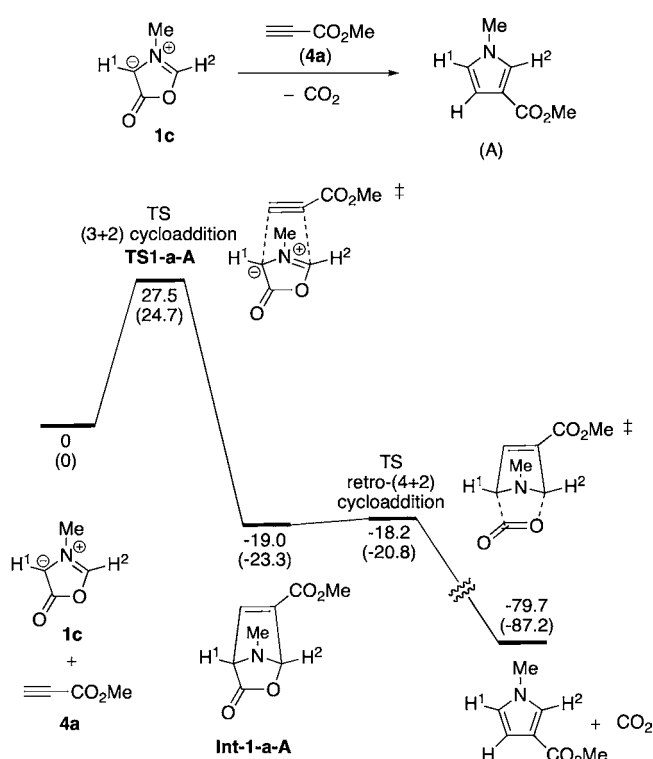


Figure 7. Free energy profile for reaction of Münchnone **1c** with electron-deficient alkyne **4a**, giving the major regioisomer of the pyrrole (**A**). Free energies in chloroform (kcal/mol) were computed at the B3LYP/6-31+G(d) level including SMD solvation energies; corresponding gas-phase free energies are included in parentheses.

distortion energies of the transition states leading to **A** are higher than those for the transition states leading to **B** because the **A** transition states display more advanced bond formation,

with greater cis bending of the alkyne and out-of-plane bending of the dipole (e.g., compare **TS1-a-A** and **TS1-a-B** in Figure 5).

On the other hand, the regioselectivity observed in the reaction of the phospho-Münchnone with methyl propiolate is traced not to the interaction energy but to the distortion energy. The phospho-Münchnone in the TS leading to **A** (**TS3-a-A**) has undergone less P–O bond contraction, and the alkyne is trans bent, which is more favorable than the cis-bent alkyne in the TS leading to **B** (**TS3-a-B**). The small distortion energy of **TS3-a-A** is also responsible for the higher overall reactivity of **3c** (compared with **1c**) toward this electron-poor alkyne.

The regioselectivities of the arylacetylene cycloadditions (Table 5) are controlled by distortion energies. The Münchnone TSs leading to pyrroles **B** benefit from distortion energies that are 4–6 kcal/mol smaller than those leading to pyrrole **A**. The small distortion energies offset these TS' weaker interaction energies, which are 2–3 kcal/mol smaller than those of the minor TSs. In the phospho-Münchnone cycloadditions, the TS distortion energies favor formation of pyrrole **A** with alkyne **4f** and pyrrole **B** with alkyne **4h**. Only in the unselective reaction of the phospho-Münchnone with phenylacetylene does the correlation of selectivity with E_{dist} break down; here E_{dist} favors **B** by 1.8 kcal/mol, while E_{int} favors **A** by an almost equal amount (2.1 kcal/mol).

Correlation between Experiment and Theory. Distortion/interaction analysis provides the first self-consistent rationale for the rates and regioselectivities of cycloadditions involving the mesoionic 1,3-dipoles. For Münchnones, FMO theory suggests a dominant orbital interaction between the HOMO(Münchnone) and LUMO(alkyne) leading to pyrrole **A**. However, experimentally, the opposite regioisomer is always competitive. The low selectivity arises because the favorable TS interaction energy in TS leading to **A** (which is large due to the nucleophilicity of the dipole) is offset by a relatively large distortion energy, associated with the more advanced bond formation in this TS. Distortion becomes increasingly important as the alkyne becomes more electron rich and is the dominant selectivity-determining factor for the arylacetylenes. The TS geometries in Figures 5 and 6 represent the two extremes of a progression of geometrical changes that occurs on going from electron-poor to electron-rich alkynes. Distortion energy trends along this series stem from a complex combination of geometrical changes, but distortion energies generally appear to be most sensitive to changes in the bond angle at the substituted alkyne terminus and the CH dihedral angle at the dipole C2 carbon, which become more distorted as the alkyne becomes more electron rich.

For phospho-Münchnones, cycloaddition regioselectivity is generally driven by distortion energy differences. Once again, the distortion energies are influenced by numerous geometrical factors, but the P–O distance and the direction of alkyne bending appear to be most important. For regioisomer **A**, the P–O distance in the TS decreases as the alkyne becomes more electron rich (e.g., compare **TS3-a-A** with **TS3-h-A**) and the alkyne changes from a favorable trans-bent geometry to a less favorable cis-bent geometry. In the **B** transition states, by contrast, the more electron-rich alkynes have less cis bending and the dipole P–O distance varies little across the series. These factors combine to cause an inversion in distortion energy differences, favoring **A** for electron-poor alkynes and **B** for electron-rich alkynes.

CONCLUSIONS

Experiments and calculations reported here provide new insights into the reactivities and selectivities of 1,3-dipolar cycloadditions involving mesoionic 1,3-dipoles. Both Münchnones and phosphamünchnones demonstrate distinct trends in alkyne cycloaddition regioselectivity. Reactivities correlate with alkyne ionization potential, while regioselectivities display an inversion as the alkyne ionization potential is raised. Frontier molecular orbital considerations do not provide a useful rationale for the selectivities or reactivities, but transition-state calculations reliably reproduce experiment and allow the observed trends to be explained in terms of the transition-state distortion and interaction energies.

To the best of our knowledge, this is the first demonstration that cycloadditions involving cyclic azomethine ylides can be performed regioselectively with both electron-rich and electron-poor alkynes without varying the C- or N-substituents on the dipole (R^1-R^3). Phosphamünchnones react regioselectively with electron-poor alkynes that do not react selectively with Münchnones, while Münchnones give better selectivities in reactions with electron-rich alkynes that do not react selectively with phosphamünchnones. These tunable selectivities suggest avenues for fruitful application to a range of other dipolarophiles, and experiments in this direction are currently underway.

EXPERIMENTAL SECTION

General Synthetic Procedures. All experiments were conducted in a Vacuum Atmospheres dry glovebox. All reagents were purchased from commercial sources and used as received. $CDCl_3$ and CD_3CN were distilled from CaH_2 under nitrogen. Acetonitrile, dichloromethane, and diethyl ether were dried with a solvent purification system. Imines were prepared as per standard literature procedures.²⁶ Alkyne **4c**²⁷ and PhP(catechyl)^{13b} were synthesized by literature procedure. Imino-Münchnone **2a** was prepared in situ. 1H and ^{13}C NMR spectra were recorded on Varian Mercury 300 and 400 MHz and Unity 500 MHz spectrometers. Pyrrole regioisomers were distinguished by a combination of NMR experiments (NOE, COSY, NOESY-2D).

Synthesis of Münchnone 1a. A modified version of a literature procedure was followed.²⁸ In the glovebox, (4- $CH_3C_6H_4$)HC=NCH₂C₆H₅ (138 mg, 0.66 mmol) and 4-methoxybenzoyl chloride (124 mg, 0.73 mmol) were mixed in 1 mL of acetonitrile and allowed to stand for 30 min. The solution was transferred to a 50 mL reaction bomb followed by Pd(^tBu₃P)₂ (34.6 mg, 10 mol %), LiBr (57.2 mg, 0.66 mmol), and *N,N*-diisopropylethylamine (119 mg, 0.92 mmol). CO (4 atm) was added to the reaction bomb, and the solution was heated at 45 °C for 16 h. After removing CO, the solution was stirred with 3 g of K₃PO₄ for 7 h in the glovebox. The solution was filtered through a small pad of Celite and concentrated to dryness. A 5 mL amount of Et₂O followed by 2.5 mL of acetonitrile were added, and the solution was stored in a -35 °C freezer for 18 h. The precipitate was collected and recrystallized with 5 mL of dichloromethane and 15 mL of pentane. The solution was left in a -35 °C freezer for 1 day, and 103 mg of pure Münchnone **1a** was collected (42% yield).

1H NMR (500 MHz, $CDCl_3$) δ (ppm): 7.51 (d, *J* = 6.5 Hz, 2H), 7.42–7.34 (m, 3H), 7.24 (d, *J* = 8.0 Hz, 2H), 7.16 (d, *J* = 7.5 Hz, 2H), 7.04 (d, *J* = 8.0 Hz, 2H), 6.88 (d, *J* = 7.0 Hz, 2H), 5.35 (s, 2H), 3.80 (s, 3H), 2.26 (s, 3H). ^{13}C NMR (125.7 MHz, $CDCl_3$) δ (ppm): 161.7, 160.8, 143.3, 136.0, 134.6, 129.6, 129.5, 129.1, 128.6, 127.7, 125.7, 125.6, 115.3, 114.9, 95.9, 55.6, 50.6, 21.2. HRMS (APCI⁺) for C₂₄H₂₂O₃N⁺: calcd 372.15942, found 372.115955.

Synthesis of Phosphamünchnone 3a. A modified version of a literature procedure was followed.^{13b} In the glovebox, (4- $CH_3C_6H_4$)-HC=NCH₂C₆H₅ (209 mg, 1.00 mmol) and 4-methoxybenzoyl chloride (179 mg, 1.05 mmol) were mixed in ca. 1 mL of acetonitrile

and allowed to stand for 30 min. An acetonitrile solution (ca. 2 mL) of PhP(catechyl) (237 mg, 1.1 mmol) was added followed by DBU (274 mg, 1.8 mmol); after 1 h, the mixture was diluted with acetonitrile to ca. 8 mL total volume and cooled at ca. -40 °C overnight to improve product precipitation. Filtration, washing with cold acetonitrile, and removal of trace solvent residues in vacuo for ca. 12 h provides 430 mg of product (77% yield).

1H NMR (500 MHz, $CDCl_3$) δ (ppm): 7.66 (dd, *J* = 8.5 Hz, 17.5 Hz, 2H), 7.44 (d, *J* = 6.5 Hz, 2H), 7.35–7.31 (m, 2H), 7.29–7.24 (m, 4H), 7.04–7.03 (m, 3H), 6.99–6.97 (m, 2H), 6.91 (d, *J* = 8.0 Hz, 2H), 6.84 (d, *J* = 8.5 Hz, 2H), 6.72 (dd, *J* = 3.0 Hz, 5.5 Hz, 2H), 6.45 (br s, 1H), 5.03 (d, *J* = 15.5 Hz, 1H), 4.92 (d, *J* = 15.5 Hz, 1H), 3.79 (s, 3H), 2.28 (s, 3H). ^{13}C NMR (125.7 MHz, $CDCl_3$) δ (ppm): 161.0, 149.3, 148.1, 145.8, 143.0 (d, $^1J_{C-P}$ = 226.5 Hz), 135.8, 135.4 (d, $^4J_{C-P}$ = 1.4 Hz), 135.2 (d, $^3J_{C-P}$ = 6.1 Hz), 132.3 (d, $^2J_{C-P}$ = 17.6 Hz), 129.7, 128.7, 128.6 (d, 2 or $^3J_{C-P}$ = 3.8 Hz), 128.1 (d, 2 or $^3J_{C-P}$ = 4.6 Hz), 128.0, 127.9, 127.6, 126.3, 121.8, 119.4, 119.0, 114.2, 110.9 (br d, $^2J_{C-P}$ = 10.7 Hz), 110.7 (br s), 73.2 (d, $^1J_{C-P}$ = 221.8 Hz), 55.5, 51.0 (d, $^3J_{C-P}$ = 8.3 Hz), 21.3 (d, $^6J_{C-P}$ = 2.4 Hz). HRMS (APCI⁺) for C₃₅H₃₁O₄NP⁺: calcd 560.19852, found 560.19901.

Cycloaddition of Alkynes with Münchnone 1a. In a screw cap NMR tube containing Münchnone **1a** (37.1 mg, 0.1 mmol) in 1 mL of dry $CDCl_3$ with an internal standard (benzyl benzoate) was added the alkyne (0.2 mmol). The reaction was followed by 1H NMR analysis until **1a** was consumed. The ratio of pyrrole regioisomers was determined by 1H NMR analysis of the crude reaction mixture. Pyrrole products were isolated by flash chromatography columns with hexanes/ethyl acetate (9/1) or toluene/ethyl acetate (9/1) as eluent.

Cycloaddition of Alkynes with Imino-Münchnone 2a. A solution of (4- $CH_3C_6H_4$)HC=N(CH₂C₆H₅) (42.0 mg, 0.2 mmol) and *p*-methoxybenzoyl chloride (40.9 mg, 0.24 mmol) in 0.3 mL of dry $CDCl_3$ was prepared in a glovebox with an internal standard (benzyl benzoate) and allowed to stand for 30 min. Cyclohexyl isocyanide (24.0 mg, 0.22 mmol) was added and let stand for 1 h, followed by K₃PO₄ (128 mg, 0.6 mmol). The solution was stirred for 1 h and then transferred to a screw cap NMR tube with the alkyne (0.6 mmol), and the final volume of dry $CDCl_3$ was adjusted to 1.8 mL. The reaction was followed by 1H NMR spectrometry until complete (1–15 days). The ratio of the regioisomers was determined by 1H NMR analysis of the crude reaction mixture.

Cycloaddition of Alkynes with Phosphamünchnone 3a. In a screw cap NMR tube containing phosphamünchnone **3a** (55.9 mg, 0.1 mmol) in 1 mL of dry $CDCl_3$ with an internal standard (benzyl benzoate) was added the alkyne (0.2–0.5 mmol). The reaction was followed by 1H NMR analysis until **3a** was consumed. The ratio of the regioisomers was determined by 1H NMR analysis of the crude reaction mixture. Pyrrole products were isolated by flash chromatography columns with hexanes/ethyl acetate (9/1) or toluene/ethyl acetate (9/1) as eluent.

Relative Reactivity of 1,3-Dipoles (Figure 2). To a dry $CDCl_3$ solution of Münchnone **1a** (37.1 mg, 0.1 mmol) and phosphamünchnone **3a** (55.9 mg, 0.1 mmol) in a screw cap NMR tube with an internal standard (1,3,5-trimethoxybenzene) was added methyl propiolate **4a** (3.4 mg, 0.04 mmol), and the final volume of $CDCl_3$ was adjusted to 1.5 mL. The reaction was followed by 1H NMR analysis for 1–2 days. The ratio of Münchnone **1a** and phosphamünchnone **3a** reacted was determined by 1H NMR spectra of the crude reaction mixture relative to the internal standard.

Relative Alkyne Reactivity (Table 3). To a dry $CDCl_3$ solution of two alkynes in a 1:1 ratio (0.5 mmol) with an internal standard (benzyl benzoate) was added Münchnone **1a** (37.2 mg, 0.1 mmol). The final volume of $CDCl_3$ was adjusted to 1.5 mL, and the mixture placed in a screw cap NMR tube. The reaction was followed by 1H NMR analysis for 1–6 days. The ratio of alkynes reacted was determined by 1H NMR spectra of the crude reaction mixture relative to the internal standard. Due to their different reactivity, a competition experiment between alkynes **4c** and **4f** was performed with a 1:9 alkyne ratio.

Computational Methods. Density functional theory calculations were performed using the Gaussian 03²⁹ and Gaussian 09³⁰ software.

Geometry optimizations, conformational searching, and vibrational frequency calculations were conducted at the B3LYP/6-31+G(d) level.³¹ The nature of each stationary point was ascertained by vibrational frequency analysis, and transition states were further verified by IRC calculations³² where appropriate. Enthalpies and free energies were obtained from the unscaled B3LYP frequencies and are quoted at 298.15 K and 1 mol/L. Solvation energies in chloroform were calculated with the SMD model.³³ Single-point electronic energy calculations were also performed at the M06-2X/6-311+G(d,p) level³⁴ for comparison to the B3LYP data. M06-2X results are provided in the Supporting Information.

■ ASSOCIATED CONTENT

Supporting Information

Supplementary experimental procedures for pyrroles A and B, characterization data, proof of regioselectivities, computational data, and complete citations for refs 29 and 30. This material is available free of charge via the Internet at <http://pubs.acs.org>.

■ AUTHOR INFORMATION

Corresponding Authors

bruce.arndtsen@mcgill.ca

e.krenske@uq.edu.au

hok@chem.ucla.edu

Present Address

[†]Institute for Research in Immunology and Cancer, Université de Montréal, Montréal, Québec H3T 1J4, Canada.

Notes

The authors declare no competing financial interest.

■ ACKNOWLEDGMENTS

We thank NSERC, CFI, and the FQRNT supported Centre for Green Chemistry and Catalysis for their financial support to B.A.A., M.S.T.M., and D.S.C. and the National Science Foundation (CHE-0548209 to K.N.H.), Australian Research Council (DP0985623 and FT120100632 to E.H.K.), and ARC Centre of Excellence for Free Radical Chemistry and Biotechnology (funding to E.H.K.). High-performance computer resources were provided by the University of Melbourne School of Chemistry, University of Queensland Research Computing Centre, and the National Computational Infrastructure National Facility in Canberra, Australia, which is supported by the Australian Commonwealth Government.

■ REFERENCES

- (1) After the acceptance of this manuscript for publication, Lopchuk, Hughes and Gribble reported a DFT treatment of the cycloadditions of Munchnones: Lopchuk, J. M.; Hughes, R. P.; Gribble, G. W. *Org. Lett.* **2013**, *15*, 5218.
- (2) Huisgen, R.; Gotthardt, H.; Bayer, H. O.; Schaefer, F. C. *Angew. Chem., Int. Ed.* **1964**, *3*, 136–137.
- (3) (a) Gribble, G. W. In *The Chemistry of Heterocyclic Compounds: Synthetic Applications of 1,3-Dipolar Cycloaddition Chemistry Toward Heterocycles and Natural Products*; Padwa, A., Pearson, H., Eds.; Wiley: New York, 2002; Vol. 45, pp 681–753. (b) Gribble, G. W. In *The Chemistry of Heterocyclic Compounds: Oxazole: Synthesis, Reactivity, and Spectroscopy*; Palmer, D., Ed.; Wiley: New York, 2003; Vol. 60, pp 473–577.
- (4) (a) Houk, K. N.; Sims, J.; Watts, C. R.; Luskus, L. *J. Am. Chem. Soc.* **1973**, *95*, 7301–7315. (b) In *Frontier Orbitals and Organic Chemical Reaction*; Fleming, I., Ed.; Wiley: New York, 1976. (c) Huisgen, R. In *1,3-Dipolar Cycloaddition Chemistry*; Padwa, A., Ed.; Wiley: New York, 1984; Vol. 1, pp 1–176. (d) Houk, K. N.; Yamaguchi, K. In *1,3-Dipolar Cycloaddition Chemistry*; Padwa, A., Ed.; Wiley: New York, 1984; Vol. 2, pp 407–450.

- (5) (a) Avalos, M.; Babiano, R.; Cabanillas, A.; Cintas, P.; Jimenez, J. L.; Palacios, J. C.; Aguilar, M. A.; Corchado, J. C.; Espinosa-Garcia, J. *J. Org. Chem.* **1996**, *61*, 7291–7297. (b) Padwa, A.; Burgess, E. M.; Gingrich, H. L.; Roush, D. M. *J. Org. Chem.* **1982**, *47*, 786–791. (c) Coppola, B. P.; Noe, M. C.; Schwartz, D. J.; Abdon, R. L., II; Trost, B. M. *Tetrahedron* **1994**, *50*, 93–116. (d) Gribble, G. W.; Pelkey, E. T.; Simon, W. M.; Trujillo, H. A. *Tetrahedron* **2000**, *56*, 10133–10140.
- (6) (a) Croce, P. D.; Ferraccioli, R.; La Rosa, C. *Tetrahedron* **1999**, *55*, 201–210. (b) Siamaki, A. R.; Arndtsen, B. A. *J. Am. Chem. Soc.* **2006**, *128*, 6050–6051. (c) Bilodeau, M. T.; Cunningham, A. M. *J. Org. Chem.* **1998**, *63*, 2800–2801.
- (7) Huisgen, R.; Funke, E.; Gotthardt, H.; Panke, H.-L. *Chem. Ber.* **1971**, *104*, 1532–1549.
- (8) Märkl, G.; Dorfmeister, G. *Tetrahedron Lett.* **1986**, *27*, 4419–4422.
- (9) (a) Dalla Groce, P.; La Rosa, C. *Heterocycles* **1988**, *27*, 2825–2832. (b) Roth, B. D.; Blankley, C. J.; Chucholowski, A. W.; Ferguson, E.; Hoefle, M. L.; Ortwine, D. F.; Newton, R. S.; Sekerke, C. S.; Sliskovic, D. R.; Wilson, M. *J. Med. Chem.* **1991**, *34*, 357–366. (c) Padwa, A.; Chen, Y. Y.; Dent, W.; Nimmesgern, H. *J. Org. Chem.* **1985**, *50*, 4006–4014. (d) Pandey, P. S.; Srinivasa Rao, T. *Bioorg. Med. Chem.* **2004**, *14*, 129–131.
- (10) (a) Padwa, A.; Lim, R.; MacDonald, J. G.; Gingrich, H. L.; Kellar, S. M. *J. Org. Chem.* **1985**, *50*, 3816–3823. (b) Texier, F.; Mazari, M.; Yebdri, O.; Tonnard, F.; Carrié, R. *Tetrahedron* **1990**, *46*, 3515–3526. (c) Okano, T.; Uekawa, T.; Morishima, N.; Eguchi, S. *J. Org. Chem.* **1991**, *56*, 5259–5262. (d) Clerici, F.; Gelmi, M. L.; Trimarco, P. *Tetrahedron* **1998**, *54*, 5763–5774.
- (11) (a) Baggi, P.; Clerici, F.; Gelmi, M. L.; Mottadelli, S. *Tetrahedron* **1995**, *51*, 2455–2466. (b) Bonati, L.; Ferraccioli, R.; Moro, G. *J. Phys. Org. Chem.* **1995**, *8*, 452–462. (c) Croce, P. D.; Ferraccioli, R.; Rosa, C. L.; Pilati, T. *J. Chem. Soc., Perkin Trans. 2* **1993**, 1511–1515. (d) Coppola, B. P.; Noe, M. C.; Hong, S. S.-K. *Tetrahedron Lett.* **1997**, *38*, 7159–7162.
- (12) (a) Roesler, P.; Fleury, J.-P. *Bull. Soc. Chim. Fr.* **1968**, 631. (b) Clerin, D.; Meyer, B.; Fleury, J. P.; Fritz, H. *Tetrahedron* **1976**, *32*, 1055–1059.
- (13) (a) St. Cyr, D. J.; Arndtsen, B. A. *J. Am. Chem. Soc.* **2007**, *129*, 12366–12367. (b) St-Cyr, D. J.; Morin, M. S. T.; Bélanger-Gariépy, F.; Arndtsen, B. A.; Krenske, E. H.; Houk, K. N. *J. Org. Chem.* **2010**, *75*, 4261–4273. (c) Krenske, E. H.; Houk, K. N.; Arndtsen, B. A.; St. Cyr, D. J. *J. Am. Chem. Soc.* **2008**, *130*, 10052–10053. (d) Morin, M. S. T.; St-Cyr, D. J.; Arndtsen, B. A. *Org. Lett.* **2010**, *12*, 4916–4919.
- (14) Eade, R. A.; Earl, J. C. *J. Chem. Soc.* **1946**, 591–593.
- (15) Morin, M. S. T.; Aly, S.; Arndtsen, B. A. *Chem. Commun.* **2013**, 49, 883–885.
- (16) Dhawan, R.; Arndtsen, B. A. *J. Am. Chem. Soc.* **2003**, *126*, 468–469.
- (17) St. Cyr, D. J.; Martin, N.; Arndtsen, B. A. *Org. Lett.* **2007**, *9*, 449–452.
- (18) See Supporting Information for experimental details.
- (19) The electronic difference in these substituents has been previously shown to not affect the regioselectivity in related cycloadditions.^{13b} Entries 3 and 6 were previously reported in ref 13b.
- (20) (a) Huisgen, R.; Li, X.; Giera, H.; Langhals, E. *Helv. Chim. Acta* **2001**, *84*, 981–999. (b) Huisgen, R. *Angew. Chem., Int. Ed. Engl.* **1970**, *9*, 751–818.
- (21) Ionization potentials were calculated using Koopmans' theorem. Values were computed at the HF/6-31G(d,p)//B3LYP/6-31+G(d) level of theory.
- (22) Knorr, R.; Huisgen, R.; Staudinger, G. K. *Chem. Ber.* **1970**, *103*, 2639.
- (23) Pross, A. *Theoretical and Physical Principles in Organic Reactivity*; Wiley: New York, 1995.
- (24) The relative rate with imino-Münchnone **2** cycloaddition was not compared with the other 1,3-dipoles as **2** exists in an equilibrium between an acyclic ketimine and a cyclic 1,3-dipole. This decreases the concentration of the reactive imino-Münchnone in solution.

- (25) (a) Ess, D. H.; Houk, K. N. *J. Am. Chem. Soc.* **2007**, *129*, 10646–10647. (b) Ess, D. H.; Houk, K. N. *J. Am. Chem. Soc.* **2008**, *130*, 10187–10198. (c) Hayden, A. E.; Houk, K. N. *J. Am. Chem. Soc.* **2009**, *131*, 4084–4089.
- (26) Lauer, R. *Chem. Rev.* **1963**, *63*, 489.
- (27) Kanner, C. B.; Pandit, U. K. *Tetrahedron* **1982**, *38*, 3597.
- (28) Dhawan, R.; Dghaym, R. D.; Arndtsen, B. A. *J. Am. Chem. Soc.* **2003**, *125*, 1474.
- (29) Frisch, M. J. et al. *Gaussian 03*, Revision E.01; Gaussian, Inc.: Wallingford, CT, 2004.
- (30) Frisch, M. J. et al. *Gaussian 09*, Revision A.02; Gaussian, Inc.: Wallingford, CT, 2009.
- (31) (a) Lee, C.; Yang, W.; Parr, R. G. *Phys. Rev. B* **1988**, *37*, 785–789. (b) Becke, A. D. *J. Chem. Phys.* **1993**, *98*, 1372–1377. (c) Becke, A. D. *J. Chem. Phys.* **1993**, *98*, 5648–5652.
- (32) (a) Gonzalez, C.; Schlegel, H. B. *J. Chem. Phys.* **1989**, *90*, 2154–2161. (b) Gonzalez, C.; Schlegel, H. B. *J. Phys. Chem.* **1990**, *94*, 5523–5527.
- (33) Marenich, A. V.; Cramer, C. J.; Truhlar, D. G. *J. Phys. Chem. B* **2009**, *113*, 6378–6396.
- (34) (a) Zhao, Y.; Truhlar, D. G. *Theor. Chem. Acc.* **2008**, *120*, 215–241. (b) Zhao, Y.; Truhlar, D. G. *Acc. Chem. Res.* **2008**, *41*, 157–167.